Thermal phonons and defects in semiconductors: The physical reason why defects reduce heat flow, and how to control it

S. K. Estreicher,[a] T. M. Gibbons, and M. B. Bebek
Physics Department, Texas Tech University, Lubbock, Texas 79409-1051, USA

(Received 16 July 2014; accepted 14 September 2014; published online 16 March 2015)

It is generally accepted that heat-carrying phonons in materials scatter off each other (normal or Umklapp scattering) as well as off defects. This assumes static defects, implies quasi-instantaneous interactions and at least some momentum transfer. However, when defect dynamics are explicitly included, the nature of phonon-defect interactions becomes more subtle. *Ab initio* microcanonical molecular-dynamics simulations show that (1) spatially localized vibrational modes (SLMs), associated with all types of defects in semiconductors, can trap thermal phonons; (2) the vibrational lifetimes of excitations in SLMs are one to two orders of magnitude longer (dozens to hundreds of periods of oscillation) than those of bulk phonons of similar frequency; (3) it is phonon trapping by defects (in SLMs) rather than bulk phonon scattering, which reduces the flow of heat; and (4) the decay of trapped phonons and therefore heat flow can be predicted and controlled—at least to some extent—by the use of carefully selected interfaces and δ layers. © *2015 AIP Publishing LLC*.
[http://dx.doi.org/10.1063/1.4913826]

I. INTRODUCTION

When a temperature gradient is applied to a material, heat is transported from the warmer to the colder regions by charge carriers and/or host-crystal (bulk) phonons. In low-doped semiconductors and at low to moderate temperatures, the material contains few free charge carriers and the phonon contribution dominates. In the present paper, we restrict ourselves to the phonon term.

The presence of defects in the material always lowers the thermal conductivity. "Defect" is used here in its most general sense, namely, anything that disrupts the ideal crystal. Thus, defects include impurities, vacancies and self-interstitials, grain boundaries, dislocations, interfaces, and even the surface of the material. The dynamical matrix of a semiconductor containing defects includes host-crystal-related (bulk) as well as defect-related normal vibrational modes.

Since the pioneering work of Peierls in the 1920s,[1] the interactions between heat flow and defects have been described and interpreted in terms of the scattering of lattice waves (the word "phonon" was introduced by Frenkel in 1932 (Ref. 2)). At the time, the emphasis was on the description of the perfect crystal and defects were considered to be perturbations. A combination of bulk phonons scatter off a defect and this generates a new combination of bulk phonons. The scattering by defects disrupts the flow of heat and reduces bulk phonon lifetimes. Klemens,[3] Ziman,[4] and Callaway[5] refined this concept. Many authors[6–11] have introduced scattering lifetimes associated with impurities, boundaries, surfaces, interfaces, and other defects when calculating thermal conductivities. Matthiessen's rule combines the sum of the inverse lifetimes associated with normal, Umklapp, grain boundary, and scattering by various types of defects. Phonon scattering has been used by so many for so long that it has become the accepted way to think about the interactions between phonons and defects.[12] But how does this scattering work at the atomic level?

A first-principles description of the processes taking place must include the normal vibrational modes associated with the defects. Phonons in these modes behave differently than phonons in bulk modes, even when they have very similar frequencies. We have discussed the following issues in Ref. 13.

(1) *Bulk modes* are delocalized in space (many and sometimes all of the host atoms oscillate together). The frequency of bulk modes has an upper limit. In silicon—the example material discussed here—the highest frequency is about 531 cm^{-1}, the Γ-phonon.[14] If a temperature gradient is applied, phonons in acoustic modes transport heat from the warmer to the colder regions of the crystal.
(2) *Defect-related modes* are localized in space. We call them Spatially Localized Modes (SLMs). The *localization* is quantified using the eigenvectors of the dynamical matrix. The frequencies of SLMs can be low (within the phonon density of states of the host) or high (for light impurities). Note that light impurities in semiconductors are often associated with high-frequency Raman or infrared (IR) active local vibrational modes,[15] a subset of high-frequency SLMs. The importance of localized modes in relation to a reduction in the thermal conductivity[16,17] and the trapping of energy by defects[18] have been reported in molecular-dynamics (MD) simulations by other authors.
(3) The *vibrational lifetimes* of high-frequency IR-active SLMs have been measured by transient-bleaching spectroscopy[19–23] and estimated from the low-temperature IR linewidth.[22] They have also been calculated using *ab initio*, non-equilibrium, microcanonical MD simulations.[23–26]

[a]Author to whom correspondence should be addressed. Electronic mail: stefan.estreicher@ttu.edu

These lifetimes vary from a few to a few hundred ps, and large isotope effects have been observed and predicted. The same theoretical approach can be used to calculate the lifetimes of phonons in low-frequency SLMs or bulk modes. The lifetimes of phonons in SLMs are much longer than those in bulk modes.

In the present contribution, we calculate the vibrational lifetimes of phonons in SLMs with high and low frequencies, and compare them to the lifetimes of bulk phonons. The results show that phonons trapped in SLMs couple to bulk phonons much less efficiently than bulk phonons couple to each other. These calculations allow us to quantify "phonon trapping" in terms of the internal clock of the oscillator: the number of periods of oscillation. Phonons in SLMs are trapped for dozens and sometimes hundreds of periods of oscillation before decaying. As a consequence, the decay does not depend on the origin of the excitation and momentum is not conserved. Instead, the decay depends on the availability of receiving modes. This is of special importance when the defect involved is the interface between two materials, which occurs at δ-layers, heterojunctions, surface layers, nanodots embedded on a substrate, as well as more complex structures such as superlattices. The decay of phonons trapped at the interface depends on the phonon densities of state of the two materials involved. The number of phonon-trapping SLMs and their decay determine the effective coefficients of thermal reflection and transmission. We predict that heat flow can be controlled by carefully selecting the materials on either side of the interface. Other groups[12,16,17] have discussed the use of interfaces to control the flow of heat but without an atomistic discussion of the underlying physical processes.

In Sec. II, we summarize the theoretical approach. In Sec. III, we compare the vibrational lifetimes of bulk and localized phonons. In Sec. IV, we discuss the decay of the phonons trapped at an interface. In Sec. V, we summarize the key results and the differences between phonon scattering and phonon trapping, and discuss some consequences.

II. THEORETICAL APPROACH

Our electronic structure calculations are performed using first-principles theory as implemented within the SIESTA[27] software package. Our *ab initio* MD simulations are microcanonical: the volume, number of particles, and total energy of the system are conserved. No thermostat is used. This is critical since vibrational modes excited above the background temperature would decay faster by coupling to the thermostat than to other modes.

All of the normal vibrational modes of the system are included in the calculations and the modes are allowed to couple to each other as they wish. The details of the method have been described elsewhere.[13,24–26,28]

The host crystal is represented by a variety of supercells ranging in size from Si_{64} to Si_{216} (3-D periodic) and from $Si_{200}H_{32}$ to $Si_{250}H_{40}$ (1-D periodic nanowires). A variety of impurities and defects are introduced into these cells. The geometries are carefully optimized so that the dynamical matrices contain no negative eigenvalues. The motion of the nuclei is calculated using classical forces obtained from total energies via the Hellmann-Feynman theorem.[29] Norm-conserving *ab initio*-type pseudopotentials are used to remove the electronic core regions from the calculations, and the electronic valence regions are treated within density-functional theory. The valence states are described using pseudo-atomic (numerical) basis sets. The basis sets are double-zeta for elements in the first two rows of the Periodic Table and polarization functions are added for 3rd-row elements. We use local density approximation in calculations involving only light elements and generalized gradient approximation when heavier elements are involved.

The MD simulations begin with the cell prepared slightly away from thermal equilibrium and we monitor all the normal vibrational modes as it returns to equilibrium. The time step is 1/40th to 1/30th of the fastest oscillation in the system, typically 0.2 to 1 fs depending on the mass of the lightest element in the cell. Supercell preparation using the eigenvectors of the dynamical matrix produces small temperature fluctuations starting with first step. The magnitude of these fluctuations remains constant for thousands of time steps (Fig. 1). Averaging over n initial random sets of normal-mode phases and energies considerably reduces the temperature fluctuations. The total energy (or temperature) of the cell remains constant (Fig. 1).

The key ingredient of supercell preparation is the dynamical matrix, which is calculated at $T = 0\,K$ with $k = 0$. The eigenvalues are the normal-mode frequencies ω_s and the orthonormal eigenvectors $e_{\alpha i}^{\ s}$ give the relative displacement of atom α along the $i = x,y,z$ directions for each mode s. They are related to the Cartesian coordinates $r_{\alpha i}$ via the normal-mode coordinate, $r_{\alpha i}(T,t) = \Sigma_s\, e_{\alpha i}^{\ s}\, q_s(T,t)/\sqrt{m_\alpha}$, where T is the temperature and t the time. The mass m_α of atom α appears because the dynamical matrix is mass weighted.

Even though the MD runs are fully anharmonic with forces obtained from the total energies, the conversion between Cartesian and normal-mode coordinates must

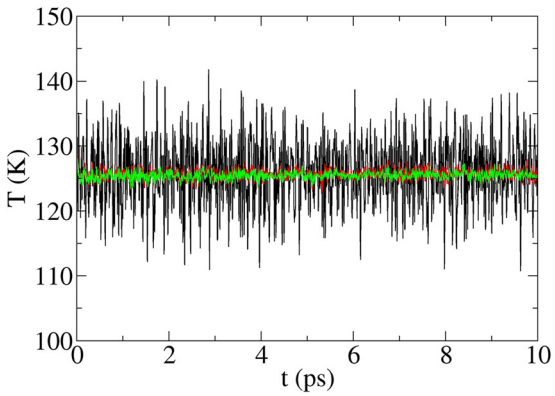

FIG. 1. MD simulation (10 000 time steps) for the $Si_{200}H_{32}$ nanowire prepared away from thermal equilibrium at the time $t = 0$ with a "hot" slice at $T_{hot} = 207\,K$ and the rest of the nanowire at $T_{cold} = 120\,K$. The cell returns to equilibrium during the MD run. The figure shows the temperature of the entire system, which remains constant at $T = 125\,K$. A single MD run (black line) produces temperature fluctuations of the order $\pm 15\,K$. Averaging over 50 (red) and 100 (green) MD runs, each with different random initial sets of mode phase and energies reduces the fluctuations to $\pm 3\,K$ and $\pm 1\,K$, respectively. This level of accuracy allows us to monitor very small changes in temperature or individual normal-mode energies and amplitudes.

involve some assumption for the unknown q_s. We use $q_s(T,t) = A_s(T)\cos(\omega_s t + \varphi_s)$, which introduces a random distribution of mode phases at the time $t = 0$. The mode amplitudes $A_s(T)$ are given by the condition that, in thermal equilibrium, the average energy per mode is $k_B T$, where k_B is the Boltzmann constant. We introduce random mode energies, which follow the Boltzmann distribution and average to $k_B T$ at the time $t = 0$.[25,28] The MD simulations must be repeated with different sets of random initial mode phases and energies and then the results are averaged.

In order to study heat flow, a thin slice of the cell is prepared at a higher temperature than the rest of the cell, but the modes are kept in phase at the interface. This is accomplished by preparing the entire cell at T_{cold}, then increasing the mode amplitudes until the atoms in the warmer slice are at the temperature T_{hot}. Then, we start the MD simulation.

The vibrational lifetime of a phonon in the normal mode s with frequency ω_s is calculated as follows. At the time $t = 0$, the supercell is prepared at the temperature T_0 except for the vibrational mode s, which is assigned the potential energy $3\hbar\omega_s/2$ (zero-point energy plus one phonon) using the appropriate eigenvector of the dynamical matrix. Thus, our classical oscillator has the same initial amplitude as the quantum-mechanical one. This potential energy slightly increases the temperature of the cell since $3Nk_B T_{cell} = (3N-1)k_B T_0 + 3\hbar\omega_s/2$, where N is the number of atoms in the cell. In Refs. 23–25, the temperature at which the lifetimes were calculated was erroneously reported to be T_0 instead of T_{cell}, a shift of $\sim$20 K in Si_{64} if $\omega_s \sim 2000\,cm^{-1}$.

Then, a random distribution of mode phases and energies is assigned (except for the mode s) and MD simulations are performed. At each time step, the 3N Cartesian coordinates of all the nuclei are converted into the 3N normal-mode coordinates, which allows us to monitor the energy and amplitude of every mode as a function of time. The MD runs are repeated n times with randomly selected initial mode phases and energies, and the lifetime is obtained from the average $\langle n \rangle$ over these runs. Because of the random distribution of mode phases and energies, strongly coupling modes are occasionally assigned above-average energies and happen to be in phase. This can result e.g., in the excited mode gaining energy instead of decaying. Such MD runs would not matter in the limit $n \to \infty$. Since we average over $n = 30$ to 100 runs, we reject these runs.

Vibrational lifetimes cannot be calculated at arbitrarily low temperatures if the nuclear dynamics are classical. Indeed, as the temperature drops, the classical amplitudes become small, all the modes harmonic and no longer couple. The calculated lifetimes become infinite. But in the quantum system, the receiving modes reach their zero-point energy state at some critical temperature below which the oscillation amplitudes, anharmonic couplings, and therefore lifetimes, remain constant. This critical temperature is in the range of $T \sim 50$ K or 75 K.[19,20] The exact value depends on the receiving modes. However, above that critical temperature, the behavior is classical and the calculated lifetimes agree with the measured ones. While each oscillator remains a quantum object at higher temperatures, IR techniques measure some $10^{16}\,cm^{-3}$ oscillators, and the average over this large number behaves classically above $T \sim 50$ K or 75 K.

III. LIFETIME OF A PHONON IN SLMS AND IN BULK MODES

Table I lists the vibrational lifetimes calculated for a few high- and low-frequency SLMs, as well as bulk phonons. In each case, the phonon is in a vibrational mode that is not populated at the selected background temperature. The lifetimes are given in ps as well as number of periods of oscillation. It is common for low-frequency vibrational excitations to exhibit more than one decay channel, each with its own lifetime. When we repeat the calculation $n \sim 50$ times or more, the decay channel associated with the shortest lifetime becomes the most frequent one.

It is often stated that localized vibrational excitations do not couple efficiently to delocalized modes. This qualitative statement is quantified here in terms of the number of periods of oscillation and can be visualized by plotting the decay of the vibrational excitations for SLMs and bulk modes of comparable frequency (Fig. 2).

TABLE I. Calculated vibrational lifetimes (in ps and number of periods of oscillations) of high-frequency IR-active SLMs for which experimental data (in parenthesis) are available as well as low-frequency SLMs and bulk modes. The asterisk indicates that the temperatures are corrected from T_0 to T_{cell} (see text). The measured lifetimes are at low temperatures. When two decay channels are possible, two lifetimes are listed. (a) is the C-H_{ab} stretch mode of CH_2*;[26] (b) is the Si-H stretch mode in the decorated divacancy V_2HD;[25] (c) is the Si-H stretch mode in V_2H_2;[19,25] (d) is the asymmetric stretch of bond-centered H_{bc}^+ (Refs. 22 and 25) (the short lifetime is an anomalous decay into SLMs instead of bulk modes[13]); (e) is the Si-D stretch mode in V_2D_2;[19,25] (f) is the asymmetric stretch of interstitial oxygen in ^{30}Si-^{16}O-^{28}Si;[23] (g) is a Si-C mode at the Si/C interface in the δ-doped $Si_{225}C_{25}H_{40}$ nanowire; (h) is a Si-H wag mode on the surface of the $Si_{250}H_{40}$ nanowire; (i) is a Si-Ge mode at the Si/Ge interface in the δ-doped $Si_{225}Ge_{25}H_{40}$ nanowire; (j) is a Si-D wag mode on the surface of the $Si_{250}D_{40}$ nanowire; (k) is a wag mode of interstitial O; (l) (the Γ mode), (n), (o), and (q) are bulk modes in Si_{64}; (m) and (p) are bulk modes in the $Si_{250}H_{40}$ nanowire.

Defect	ω (cm^{-1})	T (K)	τ (ps)	No. of periods
C-H_{ab} stretch (a)	2564 (2688)	120	2.7–4.8 (2.4)	208–369
Si-H stretch (b)	2100	225*	117	7371
Si-H stretch (c)	2092 (2072)	225*	180 (175)	11297
H_{bc}^+ stretch (d)	2014 (1998)	125*	8.7 (7.8)	526
Si-D stretch (e)	1509 (1510)	225*	106 (93)	4799
O_i stretch (f)	1183 (1133)	75*	22 (27)	781
Si-C mode (g)	556	125	11 or 17	183 or 851
Si-H wag (h)	531	125	25	404
Si-Ge mode (i)	426	125	3.5 or 6.8	45 or 87
Si-D wag (j)	368	125	4.7	52
O_i wag (k)	224	100	6.2	42
Γ phonon in Si (l)	530	125	0.2 or 0.5	3 or 7
Bulk mode (m)	424	125	0.3 or 0.8	4 or 10
Bulk mode (n)	364	125	0.1 or 0.2	1 or 2
Bulk mode (o)	242	125	0.1 or 0.2	1
Bulk mode (p)	241	125	0.2 or 0.6	1 or 4
Bulk mode (q)	127	75	0.1	0.5

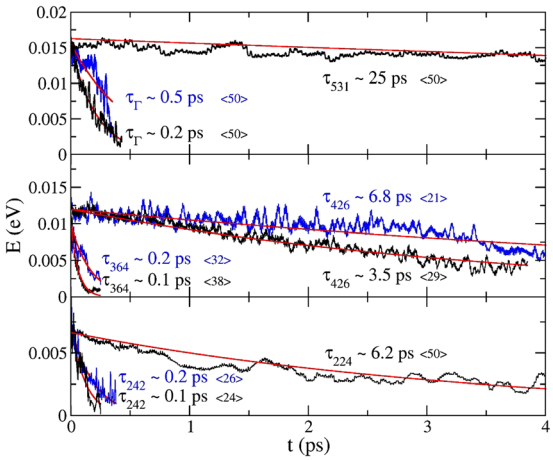

FIG. 2. Calculated decay of (top) the Si-H wag mode on the surface of the $Si_{250}H_{40}$ nanowire (531 cm^{-1}) and the Si Γ-mode in Si_{64} (530 cm^{-1}); (middle) the 426 cm^{-1} SLM in the $Si_{225}Ge_{25}H_{40}$ δ-doped nanowire and a bulk mode at 364 cm^{-1} in Si_{64}; (bottom) the interstitial O wag mode in Si_{64} (224 cm^{-1}) and a bulk mode at 242 cm^{-1} in the same supercell. The decays are averages ⟨n⟩ over n runs with different random distributions of initial mode phases and energies. Some excitations exhibit two decay channels.

Table I and Fig. 2 show that the vibrational lifetimes of delocalized (bulk) modes are systematically much shorter than those of localized (SLM) modes, regardless of their frequency. Bulk mode excitations survive at most a handful of periods of oscillations, sometimes less than a single period, while SLM excitations survive for dozens, hundreds, and in some cases thousands of periods of oscillation before decaying into bulk modes. Defect-related SLMs do not couple efficiently to bulk modes, while bulk (delocalized) modes couple to each other very quickly.

When heat flows through the material and encounters a defect, some SLMs associated with the defect trap phonons for lengths of time that can be quantified in terms of the number of periods of oscillation before they decay. Phonon trapping is an important reason why defects reduce the phonon contribution to the flow of heat. An example in clathrates has recently been reported.[30]

Since phonon trapping lasts for many periods of oscillation, the memory of the source of the excitation fades and momentum is not conserved. Too many forces are at play for too long a period of time. These bulk-phonon–defect interactions are not scattering events, as "scattering" implies quasi-instantaneous interactions and at least some momentum transfer. Instead, we have phonon trapping (usually in many SLMs) for some length of time followed by a decay into bulk mode of lower frequency.

Bulk-phonon–bulk-phonon interactions with $\hbar\omega > k_BT$ also involve phonon trapping, but the vibrational lifetimes are less than one or at most just a few periods of oscillation. Approximating such interactions in terms of (bulk) phonon scattering is much more justified.

IV. CONTROLLING HEAT FLOW WITH INTERFACES

When thermal phonons flow through a material and encounter a defect, phonon trapping occurs. The trapping itself cannot be controlled because it depends not only on the nature of the defect but also the local temperature (heat front)—that is on the location of the defect relative to a given heat source. However, the decay of the trapped phonons depends on the availability of receiving modes, not on the source of the excitation. This implies that the decay of phonons trapped at SLMs can be controlled, at least to some extent. One interesting possibility is to use interfaces (δ- or surface-layers, at nanodots in or on a substrate, superlattices, heavily doped channels, etc.).

Consider the interface between any two materials A and B. For simplicity, we define the interface as involving only those A and B atoms that are bound to each other. This definition can be generalized but the argument is the same. Thus, our system has only A-A or B-B bonds on either side of an interface consisting of A-B bonds.

Assume that heat propagates from material A towards material B, and the temperature of the heat front is T_{local}. When the heat front reaches the interface, the SLMs associated with it trap phonons up to the frequency $\omega = k_BT_{local}/\hbar$. Some of the excitations survive for a few dozen and others for a few hundred periods of oscillation. These phonons then decay into bulk modes of lower frequency. If material B consists of heavier atoms than material A, then B will contain more low-frequency receiving modes than A, and the coefficient of thermal transmission will be large. The opposite holds if the atoms in material B are lighter than those in A. Then, the coefficient of reflection will be large.

In order to illustrate this, we consider a four-atoms thick δ-layer in the $Si_{225}X_{25}H_{40}$ nanowires with X = Ge or C (Fig. 3). Following our narrow definition, the interface consists of the atoms forming Si-Ge or Si-C bonds. A thin slice of the Si on the left end of the nanowire is heated to $T_{hot} = 520$ K and the rest of the system is at the $T_{cold} = 120$ K. After equilibrium is reached, $T_{equil.}$ is about 140 K. Note that we use 1D-periodic boundary conditions in these calculations but are only interested in the heat flowing from the hot slice toward the interface. In order to stop heat flow from the nearest image slice (beyond the right end of the cell), we designed a heat barrier (the details of these calculations will be published elsewhere[31]).

We then let the heat flow and record the temperature of the interface ($T_{interface}$) and that of the two-atoms-thick Ge or C layer (T_{layer}). Figure 4 shows $T_{interface}$ vs. time. The Si-Ge

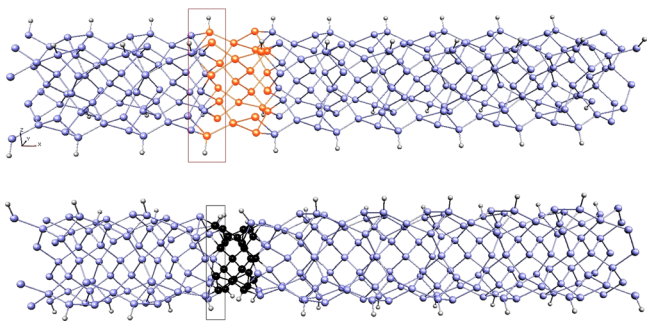

FIG. 3. In this paper, we define the Si/Ge or Si/C interface as consisting of the atoms forming Si-Ge or Si-C bonds, approximately shown by the thin boxes in the δ-doped $Si_{225}X_{25}H_{40}$ nanowire with X = Ge (top) or C (bottom). The localization of the interface vibrational modes is shown in Figs. 2 and 3 in Ref. 13.

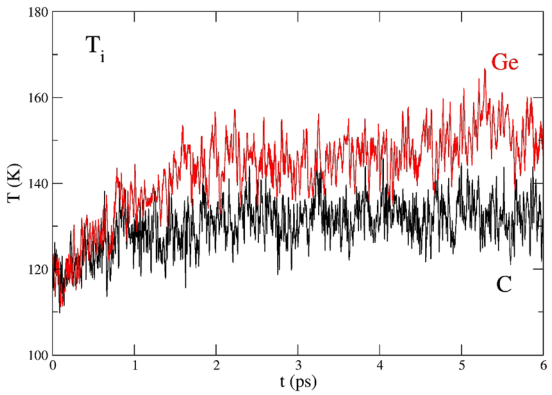

FIG. 4. Calculated temperature of the Si/Ge (red) and Si/C (black) interfaces, as defined in Fig. 3. The Si-Ge bonds have many more low-frequency SLMs than the Si-C bonds and trap more phonons. As a result, the temperature of the Si/Ge interface increases much faster than that of the Si/C interface (preliminary results).

interface traps more heat since it has many more low-frequency SLMs than the Si-C interface (the heat remains on the Si side of the δ-layer).

The trapped phonons must then decay into lower-frequency bulk modes. Since Ge is heavier than Si, and Si heavier than C, the largest number of receiving modes is in Ge, followed by Si, with precious few in C. Figure 5 shows the temperatures of the Ge and C δ-layers. The Ge layer absorbs a lot of heat (large coefficient of thermal transmission), while the C layer absorbs so little (high coefficient of thermal reflection) that its temperature remains essentially constant during the MD runs. This behavior is inconsistent with bulk phonon scattering by the interface, as momentum conservation guarantees that some heat penetrates the C layer. Thus, a diamond-like layer on a Si chip is an inefficient way to remove heat from a chip because heat would not get into it. On the other hand, a Ge layer will easily absorb energy. The details will be published elsewhere.[31]

V. SUMMARY AND DISCUSSION

We have performed microcanonical non-equilibrium MD simulations below room temperature in 3D-periodic Si supercells and 1-D periodic H-terminated Si nanowires containing a variety of defects. All the host-atom and defect-related normal vibrational modes are explicitly included in the calculations and no assumption is made relating to phonon-phonon interactions. The key findings can be summarized as follows.

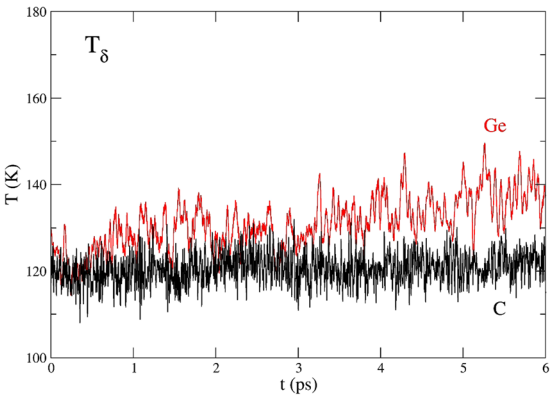

FIG. 5. Temperature of the Ge (red) and C (black) δ-layers. The phonons trapped at the Si/Ge interface (Fig. 4) decay into the low-frequency Ge modes, and the Ge temperature increases rapidly. But very few of the phonons trapped at the Si/C interface decay into C modes and the C layer remains cold. Instead, the trapped phonons decay into Si mode and the heat bounces back.

All defects we have studied (impurities, interfaces, surfaces, etc.) introduce SLMs into the phonon density of states of the material. The vibrational lifetimes of phonons in SLMs range from dozens to hundreds (sometimes thousands) periods of oscillation, while phonons in (above-background temperature) bulk modes survive for just a few periods, often less than one. Thus, phonons trap at defects and the vibrational energy remains localized at or near them for many periods of oscillation.

The decay of a trapped phonon with frequency ω_s involves bulk phonons with frequency $\omega < \omega_s$. This has practical consequences when the defect is the interface between two materials, because of the different distributions of receiving modes on the two sides of the interface. When phonons trap in SLMs at the interface, they decay preferentially into the material that has the most receiving modes. For example, a c-C layer on a Si chip is unlikely to absorb much heat at all as the heat generated in the Si will trap at the Si-C interface and then be reflected back into Si. However, a material heavier than Si, such as a Ge layer, will readily absorb it.

Our calculations do not support the assumption that defects are scattering centers for thermal phonons. We find instead that a heat front propagating through a material containing defects results in phonon trapping in SLMs for dozens or hundreds of periods of oscillation.

The physical mechanism by which defects reduce the flow of heat is phonon trapping in SLMs rather than (bulk) phonon scattering. The decay of the trapped phonons depends on the availability of receiving vibrational modes, not on the origin of the excitation. This should allow some control of heat flow using interfaces or δ layers.

Phonon scattering is qualitatively different from phonon trapping, and this has consequences. "Phonon scattering" implies quasi-instantaneous interactions, involving a time Δt comparable to a period of oscillation, and momentum is conserved. The process cannot be controlled except by trial-and-error with various defects. On the other hand, "phonon trapping" is a slow process, with $\Delta t =$ dozens or hundreds of period of oscillation, and momentum is not conserved. An analogy to phonon scattering vs. phonon trapping involves *direct* vs. *indirect* chemical reactions. In a direct reaction (e.g. $D + CH_4 \rightarrow HD + CH_3$), the scattering is *not isotropic* and momentum is conserved. In an indirect reaction (e.g. $Cl^- + CH_3Br \rightarrow CH_3Cl + Br^-$), the reactants collide, remain associated for a few ps in an intermediate ion-molecule complex (in this example, $Cl^- - CH_3Br$), the products scatter *isotropically*,[32,33] and momentum is not conserved. Phonon trapping cannot be controlled but the decay of the trapped excitations can be controlled with carefully selected interfaces or δ-layers, because the phonon densities of states of the two materials involved are known.

One example discussed above involves a c-C surface layer on Si. Since interface scattering conserves momentum, the scattering picture implies that the c-C layer will absorb heat from the Si substrate. On the other hand, phonon trapping at the Si/C interface does not conserve momentum and most of the trapped phonons will decay back into Si: The c-C layer will therefore absorb heat only very slowly.

A more interesting example involves a Ge δ-layer in a Si nanowire. If a thermal gradient is briefly applied to the nanowire, heat will propagate in the wire to the Si/Ge interface. There, phonons will trap in SLMs and then decay—mostly into the Ge layer. These phonons travel in Ge to the Ge/Si interface where they trap in SLMs, and then most of them decay back into the Ge layer. Thus, most phonons will bounce back-and-forth between the Si/Ge and the Ge/Si interfaces, with only a small number of them leaking into Si at every bounce. This situation resembles an optical cavity, but with phonons instead of photons. Thermal equilibrium will of course ultimately be achieved, but only after a substantial period of time. Such a "thermal device" could be used to trap heat for lengths of time much longer than those associated with phonon trapping, with potential applications for thermoelectric devices.

The difference between phonon scattering and phonon trapping has another consequence in the low-temperature regime, when the frequencies of the thermal phonons are lower than all the SLMs associated with a particular defect. In the phonon scattering picture, such long-wavelength (bulk) phonons are scattered by the defect. Within our description, no SLM excitation occurs and the thermal conductivity becomes independent of the defect. For example, substitutional C in Si has SLMs associated with C and its four Si nearest neighbors. These SLMs (with localization[13] L^2) are at 584 ($L^2 = 0.8$), 439 (0.3), and 419 cm^{-1} (0.2). Thus, the lowest-frequency SLM can trap a phonon at about 100 K. Below that temperature, no phonon trapping occurs and the thermal conductivity should be independent of the concentration of substitutional C in the sample. At higher temperatures, low-frequency (long-wavelength) vibrational modes are populated by multiple phonons, and thus have enough energy to excite SLMs.

Note that Si is used here as a model material and the key findings apply to a wide range of covalent materials. We did not consider high-temperatures regimes or large temperature gradients, where most vibrational modes are populated with many phonons and/or ballistic heat flow occurs. Supercell preparation relies on dynamical matrices calculated at T = 0 K. The normal-mode frequencies and the eigenvectors of the dynamical matrix become less accurate as the temperature increases. Further, the MD simulations rely on forces obtained from total energies and all entropy contributions are ignored. At this time, we simply do not know how to extend such calculations to the high-temperature regime.

ACKNOWLEDGMENTS

This work was supported in part by the grant D-1126 from the R. A. Welch Foundation. We are grateful to Texas Tech's High-Performance Computer Center for generous amounts of CPU time. Many thanks to By. Kang for producing Figure 1.

[1]R. Peierls, Ann. Phys. **395**, 1055 (1929).
[2]"Phonon" first appears on page 256 in J. Frenkel, "Wave Mechanics elementary theory" (Oxford, Clarendon, 1932) following a discussion of Tamm's 'heat quanta' or 'sound quanta' associated with Debye's 'lattice waves'.
[3]P. G. Klemens, Proc. Phys. Soc. A **68**, 1113 (1955); P. G. Klemens, in *Solid State Physics: Advances and Applications*, edited by F. Seitz and D. Turnbull (Academic, New York, 1988), Vol. 7.
[4]J. M. Ziman, *Electrons and Phonons* (Oxford, Clarendon, 1960), pp. 220–223.
[5]J. Callaway, Phys. Rev. **113**, 1046 (1959).
[6]D. A. Broido, M. Malorny, G. Birner, N. Mingo, and D. A. Stewart, Appl. Phys. Lett. **91**, 231922 (2007).
[7]M. Kazan, G. Guisbiers, S. Pereira, M. R. Correia, P. Masri, A. Bruyant, S. Volz, and P. Royer, J. Appl. Phys. **107**, 083503 (2010).
[8]A. Sparavigna, Phys. Rev. B **67**, 144305 (2003).
[9]Z. Wang and N. Mingo, Appl. Phys. Lett. **97**, 101903 (2010).
[10]M. Maldovan, J. Appl. Phys. **111**, 024311 (2012).
[11]P. Martin, A. Aksamifa, E. Pop, and U. Ravaioli, Phys. Rev. Lett. **102**, 125503 (2009).
[12]D. G. Cahill, P. V. Braun, G. Chen, D. R. Clarke, S. Fan, K. E. Goodson, P. Keblinski, W. P. King, G. D. Mahan, A. Majumdar, H. J. Maris, S. R. Phillpot, E. Pop, and L. Shi, Appl. Phys. Rev. **1**, 011305 (2014).
[13]S. K. Estreicher, T. M. Gibbons, By. Kang, and M. B. Bebek, J. Appl. Phys. **115**, 012012 (2014).
[14]F. Widulle, T. Ruf, M. Konuma, I. Silier, M. Cardona, W. Kriegseis, and V. I. Ozhogin, Solid State Commun. **118**, 1 (2001).
[15]M. Stavola, in *Hydrogen in Crystalline Semiconductors*, edited by S. J. Pearton, J. W. Corbett, and M. Stavola (Springer-Verlag, Berlin, 1991), p. 102.
[16]J. Chen, G. Zhang, and B. Li, Nano Lett. **10**, 3978 (2010).
[17]M. Hu, K. P. Giapis, J. V. Goicochea, X. Zhang, and D. Poulikakos, Nano Lett. **11**, 618 (2011).
[18]B. Deng, A. Chernatynskiy, M. Khafizov, D. H. Hurley, and S. R. Phillpot, J. Appl. Phys. **115**, 084910 (2014).
[19]M. Budde, G. Lűpke, C. Parks Cheney, N. H. Tolk, and L. C. Feldman, Phys. Rev. Lett. **85**, 1452 (2000).
[20]G. Lűpke, X. Zhang, B. Sun, A. Fraser, N. H. Tolk, and L. C. Feldman, Phys. Rev. Lett. **88**, 135501 (2002).
[21]G. Lűpke, N. H. Tolk, and L. C. Feldman, J. Appl. Phys. **93**, 2317 (2003).
[22]B. Sun, G. A. Shi, S. V. S. Nageswara Rao, M. Stavola, N. H. Tolk, S. K. Dixit, L. C. Feldman, and G. Lűpke, Phys. Rev. Lett. **96**, 035501 (2006).
[23]K. K. Kohli, G. Davies, N. Q. Vinh, D. West, S. K. Estreicher, T. Gregorkiewicz, and K. M. Itoh, Phys. Rev. Lett. **96**, 225503 (2006).
[24]D. West and S. K. Estreicher, Phys. Rev. Lett. **96**, 115504 (2006).
[25]D. West and S. K. Estreicher, Phys. Rev. B **75**, 075206 (2007).
[26]T. M. Gibbons, S. K. Estreicher, K. Potter, F. Bekisli, and M. Stavola, Phys. Rev. B **87**, 115207 (2013).
[27]D. Sánchez-Portal, P. Ordejón, E. Artacho, and J. M. Soler, Int. J. Quantum Chem. **65**, 453 (1997); E. Artacho, D. Sánchez-Portal, P. Ordejón, A. García, and J. M. Soler, Phys. Status Solidi B **215**, 809 (1999).
[28]T. M. Gibbons, By. Kang, S. K. Estreicher, and C. Carbogno, Phys. Rev. B **84**, 035317 (2011).
[29]H. Hellmann, *Einführung in die Quantenchemie* (Franz Deuticke, Leipzig, 1937), p. 285; R. P. Feynman, Phys. Rev. **56**, 340 (1939).
[30]S. Pailhès, H. Euchner, V. M. Giordano, R. Debord, A. Assy, G. Gomès, A. Bosak, D. Machon, S. Paschen, and M. de Boissieu, Phys. Rev. Lett. **113**, 025506 (2014).
[31]M. B. Bebek and S. K. Estreicher (unpublished).
[32]R. D. Levine and R. B. Bernstein, *Molecular Reaction Dynamics and Chemical Reactivity* (Oxford University Press, Oxford, 1987).
[33]J. Mikosch, S. Trippel, C. Eichhorn, R. Otto, U. Lourderaj, J. X. Zhang, W. L. Hase, M. Weidemüller, and R. Wester, Science **319**, 183 (2008).